doi:10.1016/S0022-2836(02)00400-X available online at http://www.idealibrary.com on IDEAL® J. Mol. Biol. (2002) 320, 85–95

JMB

Evolution of an Antibiotic Resistance Enzyme Constrained by Stability and Activity Trade-offs

Xiaojun Wang, George Minasov and Brian K. Shoichet*

Department of Molecular Pharmacology and Biological Chemistry, Northwestern University School of Medicine 303 East Chicago Avenue Chicago, IL 60611-3008, USA

*Corresponding author

Pressured by antibiotic use, resistance enzymes have been evolving new activities. Does such evolution have a cost? To investigate this question at the molecular level, clinically isolated mutants of the β-lactamase TEM-1 were studied. When purified, mutant enzymes had increased activity against cephalosporin antibiotics but lost both thermodynamic stability and kinetic activity against their ancestral targets, penicillins. The X-ray crystallographic structures of three mutant enzymes were determined. These structures suggest that activity gain and stability loss is related to an enlarged active site cavity in the mutant enzymes. In several clinically isolated mutant enzymes, a secondary substitution is observed far from the active site (Met182 → Thr). This substitution had little effect on enzyme activity but restored stability lost by substitutions near the active site. This regained stability conferred an advantage *in vivo*. This pattern of stability loss and restoration may be common in the evolution of new enzyme activity.

Keywords: protein stability; TEM-1; β-lactamase; antibiotic resistance; evolution

Introduction

As new antibiotics are introduced, drug-inactivating resistance enzymes have co-evolved, broadening their activity to ever more elaborate antibiotics. Does the evolution of enzymes with new substrate spectra have a cost? It is conceivable, for instance, that gaining activity against a new substrate might come at the expense of older substrates. From a structural standpoint, creating a more versatile active site could destabilize the enzyme. Unlike the well-packed, stability-conferring cores of proteins, active sites are necessarily poorly packed[1] and enlarging them would aggravate this. Also, active sites are pre-organized to recognize substrates,[2] and this pre-organization appears to introduce strain. In active sites, groups bearing the same formal charge are juxtaposed,[3,4] introducing electrostatic repulsion, and conformational strain is often observed among ligand-binding residues.[5] Consequently, it has been possible to make substitutions in active sites that result in highly stabilized mutant enzymes with reduced activity.[6–9] By the same logic, the increased activity of the mutant resistance enzymes might increase active-site strain, reducing enzyme stability. Such trade-offs between enzyme activity and stability would act as a constraint on the evolution of new resistance enzymes.

We turned to gain-of-function mutants of TEM-1 β-lactamase, the predominant source of resistance to penicillins in bacteria. The wild-type (WT) enzyme is an excellent penicillinase but has little activity against third generation cephalosporins, such as ceftazidime (CAZ) or cefotaxime (CTX). Such cephalosporins possess bulky oxyimino side-chains that are thought to be too large for the TEM-1 active site (Figure 1(a)).[10,11] Since the introduction of these drugs in 1983, mutant extended spectrum β-lactamase (ESBL) TEM enzymes have been found that confer resistance to these drugs in clinical isolates. There are now more than 50 ESBL TEM mutants and more than 18 ESBL mutants of a related SHV β-lactamase†;[12] most of these mutants consist of substitutions at a small number of residues.

In early studies, Frere and colleagues[13] showed that at least some mutant TEM enzymes had

Abbreviations used: WT, wild-type; ESBL, extended spectrum β-lactamase; IRT, inhibitor resistance TEM; RT, room temperature; FAP, 6-furylacrylpenicillanic acid; CAZ, ceftazidime; CTX, cefotaxime.

E-mail address of the corresponding author: b-shoichet@northwestern.edu

† http://www.lahey.org/studies/webt.htm

0022-2836/02/$ - see front matter

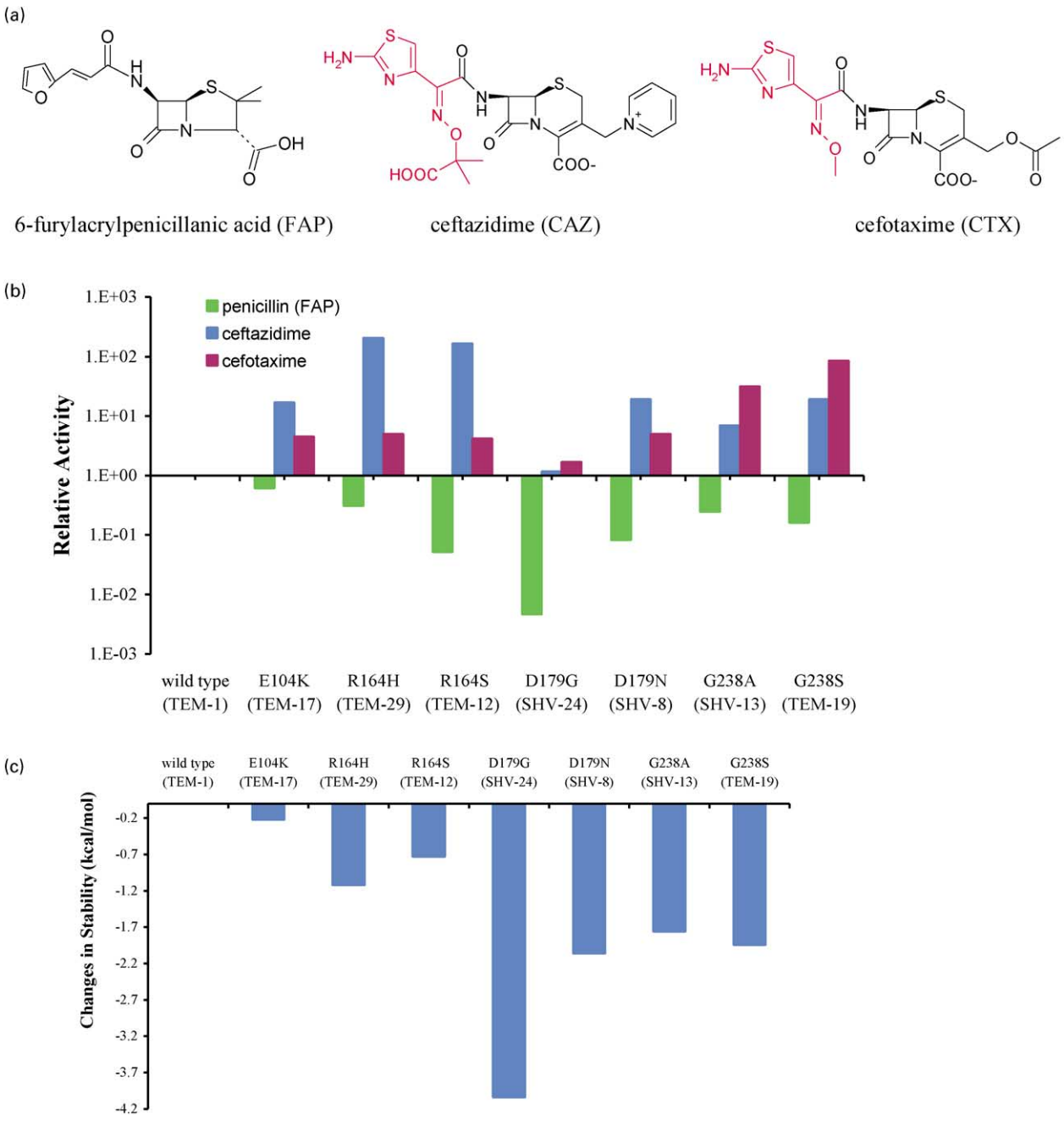

Figure 1 (*legend opposite*)

reduced stabilities relative to the WT enzyme, which seemed like an intriguing result. Here, we make all the single-site substitutions previously isolated in hospitals that confer ESBL status to TEM and/or SHV enzymes. We also make six multi-site ESBL mutant enzymes, three on the WT background and their three counterparts on an M182T background. The Met182 → Thr substitution was intriguing to us; it occurs frequently in mutant enzymes isolated in hospitals and has been reported as a rescue substitution for enzyme expression levels.[14,15] All mutant enzymes were purified to homogeneity and their kinetics investigated against a penicillin substrate and against two third-generation cephalosporin substrates. The stability of the mutant enzymes was determined thermodynamically, by two-state reversible thermal denaturation, and was investigated in cell culture experiments. To investigate the bases of the stability and activity changes at atomic resolution, the structures of three mutant enzymes were determined by X-ray crystallography. From these studies emerges a pattern of activity–stability trade-offs as TEM evolves.

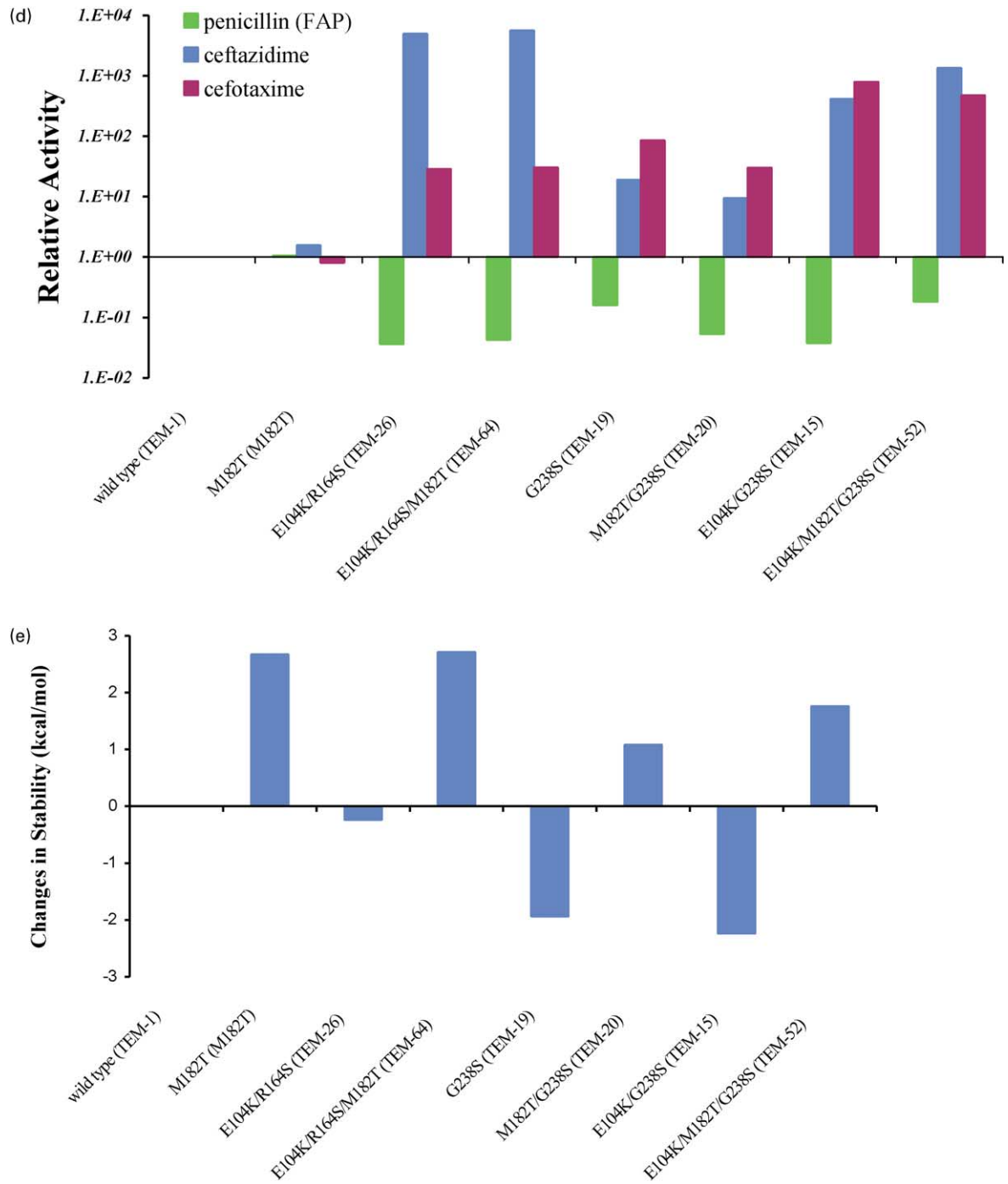

Figure 1. Relative enzyme activities and thermodynamic stabilities of TEM ESBL mutants. (a) Chemical structures of a penicillin (FAP) and two third-generation cephalosporins (CAZ and CTX). The oxyimino side-chains of CAZ and CTX are colored in red. (b) Relative activities of single-site TEM ESBLs compared to TEM-1 WT against the penicillin FAP (green bars; log scale), CAZ (blue bars) and CTX (brown bars). Relative activity is the ratio of the mutant's k_{cat}/K_M value to that of WT (a value larger than 1 indicates that the mutant is more active than WT). (c) The differential stabilities of single TEM ESBL mutants relative to WT. (d) Relative activities of mutants constructed on WT and M182T backgrounds compared to WT against FAP (green bars; log scale), CAZ (blue bars) and CTX (brown bars). (e) The differential stabilities of ESBL mutants on WT and M182T backgrounds.

Results and Discussions

Activity and stability trade-offs

Seven ESBL point mutants (e.g. TEM-19, G238S) and five multi-site mutants (e.g. TEM-15, E104K/G238S), all of which were first identified in hospital isolates, were made by site-directed mutagenesis and purified to homogeneity. The k_{cat} and K_M values of these mutant TEM enzymes were determined *versus* a penicillin, 6-furylacrylpenicillanic acid (FAP), and two third-generation

Table 1. Kinetic parameters of TEM single-site ESBL mutants

Mutants	Substrate	k_{cat} (s^{-1})	K_M (μM)	k_{cat}/K_M (s^{-1} M^{-1})
WT (TEM-1)	FAP	1210 ± 70	29.0 ± 5.5	4.18×10^7
	CAZ	0.0179 ± 0.0027	557 ± 123	3.21 × 10
	CTX	0.636 ± 0.090	308 ± 77	2.07×10^3
E104K (TEM-17)	FAP	499 ± 36	19.5 ± 3.7	2.56×10^7
	CAZ	0.408 ± 0.036	760 ± 96	5.37×10^2
	CTX	9.25 ± 1.90	980 ± 256	9.44×10^3
R164H (TEM-29)	FAP	132 ± 7	10.2 ± 1.9	1.30×10^7
	CAZ	9.23 ± 2.45	1410 ± 440	6.56×10^3
	CTX	3.43 ± 0.26	260 ± 40	1.32×10^4
R164S (TEM-12)	FAP	26.1 ± 3.0	12.1 ± 2.5	2.16×10^6
	CAZ	8.47 ± 2.54	1600 ± 570	5.28×10^3
	CTX	1.76 ± 0.13	201 ± 34	8.75×10^3
D179G (SHV-24)	FAP	4.27 ± 0.26	22.0 ± 3.4	1.94×10^5
	CAZ	0.126 ± 0.022	3350 ± 1860	3.76 × 10
	CTX	1.24 ± 0.07	350 ± 36	3.54×10^3
D179N (SHV-8)	FAP	35.0 ± 3.0	10.2 ± 2.9	3.44×10^6
	CAZ	0.0336 ± 0.0027	54.7 ± 18.5	6.14×10^2
	CTX	3.57 ± 0.19	341 ± 32	1.05×10^4
G238A (SHV-13)	FAP	187 ± 11	18.3 ± 3.4	1.02×10^7
	CAZ	0.667 ± 0.249	3010 ± 1290	2.22×10^2
	CTX	65.8 ± 8.5	1010 ± 176	6.55×10^4
G238S (TEM-19)	FAP	27.8 ± 0.7	4.15 ± 0.51	6.70×10^6
	CAZ	0.548 ± 0.133	897 ± 301	6.10×10^2
	CTX	41.8 ± 2.0	234 ± 25	1.78×10^5

cephalosporins (Tables 1 and 3). All of the ESBLs had reduced penicillinase activity, typically by ten-fold to 100-fold relative to WT. Conversely, the cephalosporinase activities typically increased 100-fold (Figure 1(b)), which is consistent with their ESBL status.

All of these ESBL mutant enzymes had lower thermodynamic stabilities relative to WT as measured by reversible, two-state thermal denaturation (Tables 2 and 4; Figure 1(c)).[13,16] Their temperatures of melting (T_m) were decreased by between 0.5 °C (for TEM-17, E104K) and 9.4 °C (for D179G, the TEM analog of SHV-24), which translate into stability losses of 0.2 to 4.0 kcal mol^{-1} (1 cal = 4.184 J) (Tables 2 and 4; Figure 1(c)). These results are consistent with the hypothesis that the newly evolved activity *versus* the third-generation cephalosporins is at the cost of the enzyme's ancestral activity and its intrinsic protein stability.

Like most enzymes, TEM-1 is marginally stable, and only so much stability can be sacrificed before a mutant ESBL will unfold at physiological temperatures. To restore stability to the ESBL mutant enzymes, a secondary substitution might have occurred. A good candidate was Met182 → Thr, which is a rescue substitution for several TEM mutants that have low expression levels in bacteria.[14,15] This substitution has been found in several hospital isolates and has been discovered repeatedly by *in vitro* evolution studies.[14,15,17] Intriguingly, in clinical isolates this substitution occurs only in combination with other ESBL substitutions or inhibitor resistance TEM (IRT) substitutions, never by itself.

To investigate the role of M182T, three naturally occurring ESBL substitutions were made on both WT and M182T backgrounds (Table 3; Figure 1(d)). The mutant enzyme M182T had activity similar to that of WT against the penicillin (FAP) and the third-generation cephalosporins CAZ and CTX (Table 3; Figure 1(d)). Thus, by itself, M182T appears to confer no functional advantage, which might be why it has not been identified clinically. Also, ESBLs constructed on an M182T background (e.g. TEM-20, G238S/M182T) had similar substrate profiles and activities compared

Table 2. Thermodynamic parameters of TEM single-site ESBL mutants

Mutant	T_m (°C)	ΔH_{VH} (kcal mol^{-1})	ΔT_m (°C)	$\Delta\Delta G_u$ (kcal mol^{-1})
WT (TEM-1)	51.5 ± 0.1	139.5 ± 7.9	–	–
E104K (TEM-17)	51.0 ± 0.1	132.3 ± 2.6	−0.5 ± 0.1	−0.22 ± 0.04[a]
R164H (TEM-29)	48.9 ± 0.2	107.6 ± 3.0	−2.6 ± 0.2	−1.12 ± 0.10
R164S (TEM-12)	49.8 ± 0.1	104.1 ± 22.9	−1.7 ± 0.1	−0.73 ± 0.05
D179G (SHV-24)	42.2 ± 0.2	51.4 ± 4.1	−9.4 ± 0.2	−4.04 ± 0.21
D179N (SHV-8)	46.7 ± 0.2	83.9 ± 2.9	−4.8 ± 0.2	−2.06 ± 0.13
G238A (SHV-13)	47.4 ± 0.2	112.4 ± 4.7	−4.1 ± 0.2	−1.76 ± 0.12
G238S (TEM-19)	47.0 ± 0.2	103.7 ± 4.7	−4.5 ± 0.2	−1.94 ± 0.12

[a] Errors propagated based on ΔH_{VH}, ΔT_m, and the Schellman equation,[35] used to calculate $\Delta\Delta G_u$ ($\Delta\Delta G_u = \Delta T_m \Delta S^{WT}$). We note that in cases where $\Delta\Delta H_{VH}$ or ΔT_m are large in magnitude, this equation breaks down and the error will be underestimated. See the discussion in Methods.

Table 3. Kinetic parameters of TEM-M182T ESBL mutants

Mutants	Notation	Substrate	k_{cat} (s^{-1})	K_M (μM)	k_{cat}/K_M ($s^{-1}\,M^{-1}$)
WT	TEM-1	FAP	1210 ± 70	29.0 ± 5.5	4.18×10^7
		CAZ	0.0179 ± 0.0027	557 ± 123	3.21×10
		CTX	0.636 ± 0.090	308 ± 77	2.07×10^3
M182T	M182T	FAP	909 ± 51	20.5 ± 4.1	4.44×10^7
		CAZ	0.0159 ± 0.0059	319 ± 129	4.99×10
		CTX	9.25 ± 1.90	980 ± 256	9.44×10^3
E104K/R164S	TEM-26	FAP	17.7 ± 1.5	11.6 ± 3.0	1.53×10^6
		CAZ	33.9 ± 4.7	207 ± 63	1.63×10^5
		CTX	3.79 ± 0.20	62.8 ± 11.4	6.04×10^4
E104K/R164S/**M182T**	TEM-64	FAP	22.0 ± 1.0	12.3 ± 1.8	1.79×10^6
		CAZ	71.3 ± 15.9	393 ± 147	1.81×10^5
		CTX	1.49 ± 0.03	23.3 ± 3.5	6.39×10^4
G238S	TEM-19	FAP	27.8 ± 0.7	4.15 ± 0.51	6.70×10^6
		CAZ	0.548 ± 0.133	897 ± 301	6.10×10^2
		CTX	41.8 ± 2.0	234 ± 25	1.78×10^5
G238S/**M182T**	TEM-20	FAP	10.8 ± 0.6	4.83 ± 1.17	2.23×10^6
		CAZ	0.148 ± 0.01	492 ± 47	3.01×10^2
		CTX	15.8 ± 1.0	250 ± 32	6.31×10^4
E104K/G238S	TEM-15	FAP	8.08 ± 0.72	5.11 ± 2.33	1.58×10^6
		CAZ	7.37 ± 1.64	806 ± 260	9.14×10^3
		CTX	29.9 ± 0.8	17.9 ± 5.4	1.67×10^6
E104K/**M182T**/G238S	TEM-52	FAP	19.9 ± 0.6	2.60 ± 0.52	7.67×10^6
		CAZ	15.3 ± 2.5	360 ± 115	4.25×10^4
		CTX	56.4 ± 3.0	54.7 ± 11.6	1.03×10^6

to their counterparts on WT backgrounds (e.g. TEM-19, G238S; Table 3; Figure 1(d)). Conversely, the effect of Met182 → Thr on stability was dramatic. M182T itself was 6.2 °C (2.7 kcal mol^{-1}) more stable than WT (Table 4; Figures 1(e) and 2). The substitution stabilized all of the naturally occurring ESBL mutants measured by 3.0 to 4.0 kcal mol^{-1} as compared to the same ESBL mutants lacking the Met182 → Thr substitution. Thus, Met182 → Thr, which is located 14.5 Å from the active site, acts as a global stabilizer that does not affect β-lactamase activity.

Stability as selection criterion *in vivo*

Frere and colleagues showed that the thermal stability loss of some ESBL is correlated with their *in vitro* susceptibilities to proteolysis,[13] which might affect their *in vivo* activities. To investigate whether increased stability confers an *in vivo* advantage, plasmids encoding the ESBL mutants with and without M182T were transformed into *Escherichia coli*. Resistance was measured in disk diffusion assays at 42 °C, 37 °C, and at room temperature (RT) against ampicillin, CAZ, and CTX (Table 5; Figure 3). At RT, no significant difference was observed between bacteria expressing enzymes containing Met182 → Thr and those expressing the same enzymes that lacked this substitution (Table 5). At 42 °C, all three ESBLs on the M182T background had significantly smaller inhibition halos, indicating higher third-generation cephalosporinase activities, than the same enzymes on the WT background (Figure 3; Table 5). The same trend was observed at 37 °C, although the effect was smaller. Since Met182 → Thr had little effect on either enzyme kinetics or *in vivo* resistance at RT, the increased resistance at higher temperatures by the constructs containing Met182 → Thr is explained most simply by their increased stabilities. A role for Met182 → Thr in promoting proper folding and disfavoring aggregation of the ESBLs cannot be ruled out.[15]

Structural bases of activity gain and stability loss

Can the increased activity and decreased stability of the ESBL mutants be attributed to a larger or more strained active site? To investigate this

Table 4. Thermodynamic parameters of TEM-M182T ESBL mutants

Mutant	Notation	T_m (°C)	ΔH_{VH} (kcal mol^{-1})	ΔT_m[a] (°C)	$\Delta\Delta G_u$[a] (kcal mol^{-1})
WT	TEM-1	51.5 ± 0.1	139.5 ± 7.9	–	–
M182T	M182T	57.7 ± 0.1	160.3 ± 4.3	6.2 ± 0.1	2.67 ± 0.13
E104K/R164S	TEM-26	50.9 ± 0.2	100.0 ± 8.8	−0.6 ± 0.2	−0.26 ± 0.09
E104K/R164S/**M182T**	TEM-64	57.8 ± 0.1	128.9 ± 2.9	6.3 ± 0.1	2.71 ± 0.13
G238S	TEM-19	47.0 ± 0.2	103.7 ± 4.7	−4.5 ± 0.2	−1.94 ± 0.12
M182T/G238S	TEM-20	54.0 ± 0.1	126.5 ± 3.2	2.5 ± 0.2	1.08 ± 0.107
E104K/G238S	TEM-15	46.3 ± 0.2	106.9 ± 5.5	−5.2 ± 0.2	−2.24 ± 0.13
E104K/**M182T**/G238S	TEM-52	55.6 ± 0.1	107.2 ± 2.7	4.1 ± 0.1	1.76 ± 0.09

[a] Changes in (Δt_m) and free energies ($\Delta\Delta G_u$) are relative to WT.

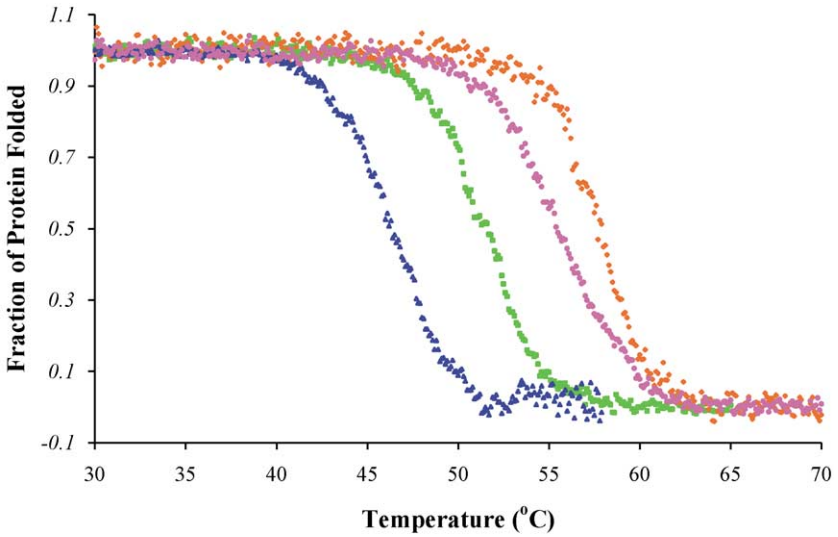

Figure 2. Representative thermal denaturation curves: WT (green squares), M182T (orange diamonds), TEM-15 (E104K/G238S, blue triangles), and TEM-52 (E104K/M182T/G238S, pink circles).

question, the structures of three mutant enzymes, M182T, G238A (the TEM equivalent of the ESBL SHV-13), and TEM-64, were determined by X-ray crystallography to 1.75, 1.85, and 1.80 Å resolution, respectively (Figures 4 and 5; Table 6). In both G238A and TEM-64, the active site enlarges compared to the WT structure (Figure 5). A superposition of WT with G238A shows that the substituted alanine residue would sterically clash with the main-chain oxygen atom of Asn170, causing the main chain of the mutant enzyme to move by 0.5 Å in this region (Figure 5(a)). This movement enlarges the active site in the region where oxyimino group of third-generation cephalosporins would be expected to bind. The increase in size of the active site is even more striking in TEM-64 (E104K/R164S/M182T). The substitution Arg164 → Ser loses one hydrogen bond with Asp179, one with Glu171, and introduces a packing defect. Consequently, Asn170 flips by almost 180° (the C^{α} atom moves by 4.5 Å), filling the cavity created by the substitution of the bulky arginine residue by the much smaller serine residue (Figures 4(b) and 5(b)). In turn, what had been a short helix in the region of residue 170 unwinds, leaving a large cavity in the active site. Qualitatively, this effect resembles one anticipated based on the simulation reported by Mobashery and colleagues,[18,19] who noted that Arg164 substitution would open a cavity in the binding site, and that the mutant enzyme had a lower helical content, on the basis of the CD signal. Consistent with the structure of TEM-52,[17] the increased activity of G238A and TEM-64 appears to be a result of enlarged binding sites that can accommodate the bulky oxyimino side-chains of the third-generation cephalosporins (Figure 1). These enlarged sites cost the mutant enzymes their intrinsic stabilities, either through strain or by giving up formerly favorable interactions. Moreover, the enlarged sites may be less suited to the smaller side-chains of penicillins, which fit snugly into the WT site.

We note that both TEM-64 and G238A were crystallized in the presence of boronic acid transition-state analogs, compounds **1** and **2** (Figure 4(c) and (d)), respectively, from Caselli *et al*.[20] In principle, these compounds could affect the conformations that we observe in these complexes. We do not believe that their effect will be significant, for several reasons. First, in the case of M182T, the crystallographic structures of both the apo and

Table 5. Resistance to third-generation cephalosporins by ESBLs on WT and M182T background at 42 °C, 37 °C, and RT in disk diffusion assays

		Halo diameter (mm)					
		42 °C		37 °C		RT	
Mutant	Notation	CAZ	CTX	CAZ	CTX	CAZ	CTX
No plasmid		32	39	34	40	52	62
Wild-type	TEM-1	29	36	31	40	46	56
M182T	M182T	28	36	31	40	48	57
E104K/R164H	TEM-26	8	30	7	25	7	40
E104K/R164H/**M182T**	TEM-64	6	22	7	24	7	39
G238S	TEM-19	31	34	28	29	35	31
M182T/G238S	TEM-20	23	23	23	23	34	33
E104K/G238S	TEM-15	28	31	19	20	20	17
E104K/**M182T**/G238S	TEM-52	16	18	14	16	20	16

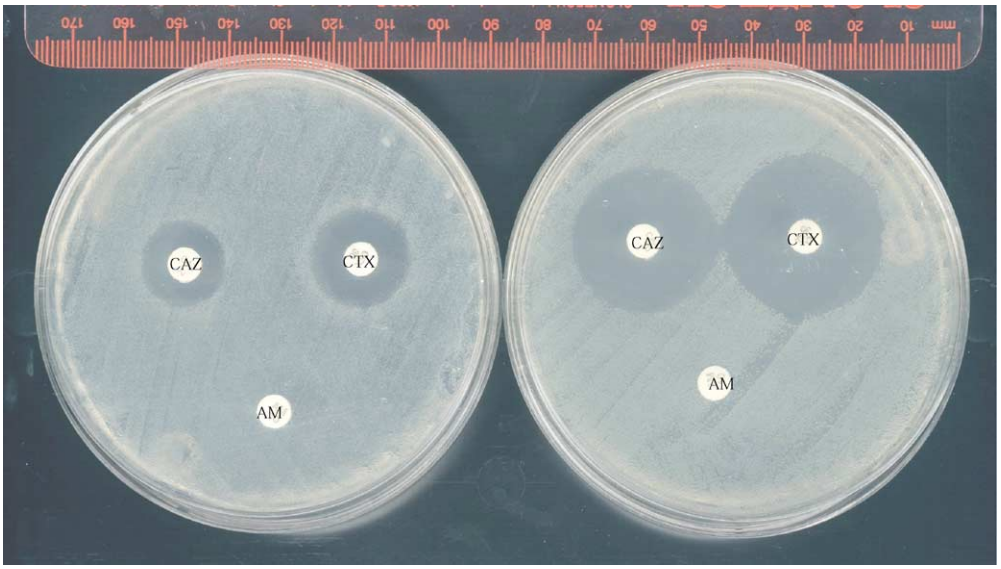

Figure 3. Comparing the *in vivo* stabilities of TEM-52 (E104K/**M182T**/G238S, left) and TEM-15 (E104K/G238S, right) at (a) 42 °C and (b) RT. Plates are representative of five independent assays for each mutant. The two top disks on each plate are CAZ and CTX from left to right, and the bottom disk is AM.

analog enzyme complexes were determined and were found to be very similar (C^{α} rms of 0.20 Å). Second, in the TEM-64 complex, the closest ligand atom is 6.1 Å away from the omega loop, which is the region that undergoes a dramatic conformational change, suggesting that no direct interaction occurs. The changed conformation of the omega loop in TEM-64 is consistent with a CD study on a similar mutant enzyme, R164N.[19] Moreover, crystal structures of TEM-52 and an ESBL mutant enzyme P54 (D179N of the class A β-lactamase PC1)[17,21] showed either similar enlargement of the active site or a disordered omega loop, which is consistent with enlargement, in their apo forms.

These ESBL mutant enzymes regain stability through the functionally neutral substitution Met182 → Thr, a residue far from the active site. How does this substitution stabilize the enzymes? In the X-ray crystal structure of M182T, the threonine residue appears better suited to the hydrophilic environment in the region, directly hydrogen-bonding with the backbone nitrogen atom of residue Ala185 and allowing newly recruited water molecules to hydrogen bond with residue Glu63 (Figure 4(c)). Such interactions are impossible with the WT methionine residue. We note that the conformation of the substituted threonine residue in the structures of both M182T and of TEM-64 differs from that adopted in the TEM-52 crystal structure.[17] This could be due to a different environment in TEM-52, or to ambiguities present in the lower-resolution TEM-52 structure. Two analogous threonine residues, one present in the related PC1 β-lactamase structure[22] and another (Thr226) present in a class C AmpC β-lactamase,[20] adopt conformations similar to that seen in TEM-64 and M182T.

Table 6. Crystal data and refinement parameters for M182T, G238A, and TEM-64 (E104K/R164S/M182T)

Mutant	M182T	G238A[a]	TEM-64[a]
Space group	$P2_12_12_1$	$P2_12_12_1$	$P2_12_12_1$
Unit cell dimensions (Å)	$a = 41.47$; $b = 61.69$; $c = 89.21$	$a = 41.37$; $b = 61.67$; $c = 89.40$	$a = 72.00$; $b = 34.55$; $c = 105.49$
Temperature (K)	100	100	100
Wavelength (Å)	1.0000	1.0000	1.0000
Beamline/detector		APS DND-CAT 5-ID/MARCCD	
Resolution (Å) (last shell)	20.0–1.75 (1.81–1.75)	20.0–1.85 (1.92–1.85)	20.0–1.80 (1.86–1.80)
No. of unique refl.	22,408 (2202)	20,097 (1959)	25,031 (2445)
Date completeness (%)	93.5 (93.3)	99.9 (99.6)	99.9 (99.9)
R_{merge} (%)	4.1 (22.5)	6.4 (12.1)	9.7 (28.0)
No. protein atoms	2027	2052	2057
No. solvent molecules	296	434	342
R_{cryst}/R_{free} (%)[b]	18.6/22.0	16.5/20.3	16.8/18.9
rms bonds (Å)	0.009	0.009	0.009
rms angles (deg.)	1.46	1.54	1.56

[a] Crystals of TEM-64 and G238A were grown with the presence of 2.5 mM boronic transition-state analog, compound **1** and **2**, respectively.[20]

[b] R_{free} was calculated with 10% of reflections set aside randomly.

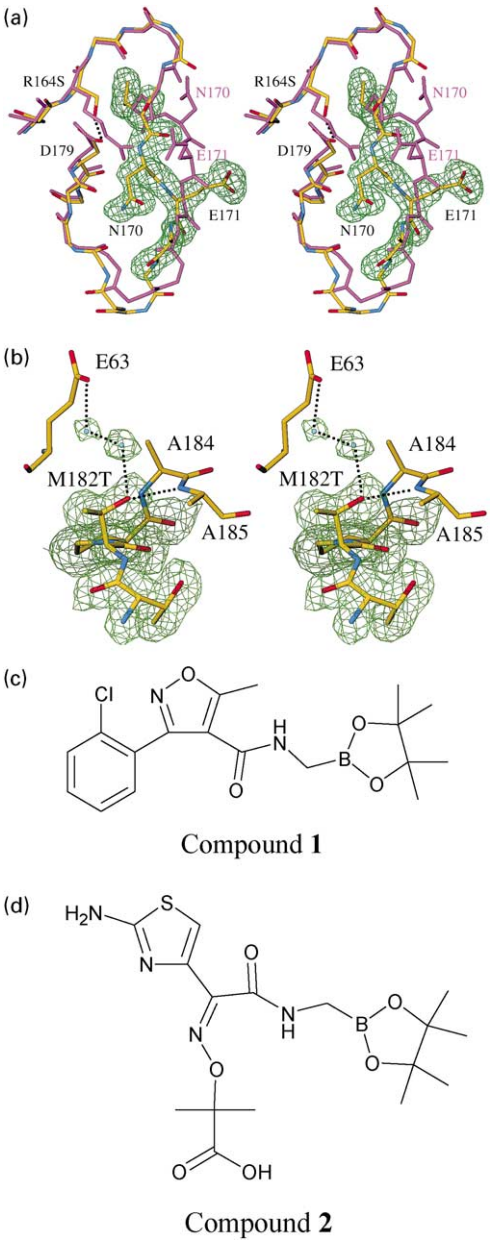

Figure 4. Crystal structures of mutant enzymes. (a) A stereo view of the superposition of the M182T (magenta) and TEM-64 crystal structures (rms is 0.83 Å for all C^{α} atoms). The key residues of the omega loop region of TEM-64 and M182T are shown. A simulated annealing $|F_o - F_c|$ omit electron density map contoured at 3σ is shown in green. Atoms of selected TEM-64 residues are colored yellow, blue, and red for carbon, nitrogen, and oxygen, respectively; and a hydrogen bond is drawn as a broken line. (b) A stereo drawing of the region around the substituted residue 182 in M182T. A simulated annealing $|F_o - F_c|$ omit electron density map contoured at 3σ is shown in green. (c) The chemical structure of compound **1**. (d) The chemical structure of compound **2**.

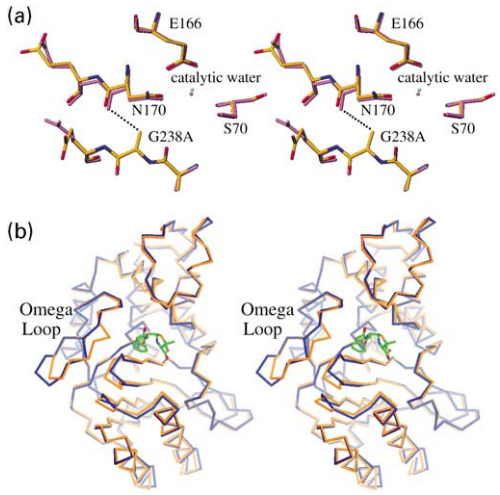

Figure 5. A stereo view of the enlarged active sites of (a) G238A and (b) TEM-64 (E104K/R164S/M182T). (a) Superposition of the G238A (carbon atoms colored orange) and WT (magenta, PDB 1XPB[39]) crystal structures (rms is 0.24 Å for all C^{α} atoms). A broken line indicates the putative steric clash (distance 2.96 Å) between the C^{β} atom of Ala238 and the carbonyl oxygen atom of Asn170 that would occur in WT. For G238A, carbon, nitrogen, and oxygen atoms are colored yellow, blue, and red, respectively. The catalytic water molecule in WT (magenta) and G238A (cyan) is shown. (b) Superposition of the C^{α} atom of TEM-64 (blue) and penicillin-bound TEM-1 E166N (orange, PDB 1FQG[33]) crystal structures (rms is 0.85 Å for all C^{α} atoms). The penicillin G acyl-adduct is shown to identify the active site. The carbon atoms in penicillin G are colored green, nitrogen atoms blue, oxygen atoms red, and the sulfur atom yellow.

A model for stability as a constraint in enzyme evolution

Under the pressure of third-generation cephalosporins, TEM ESBLs have been selected for larger active sites to accommodate the bulky side-chains of these β-lactams. In carving out a larger active site, these enzymes have lost some of penicillinase activity of WT TEM-1 and have lost internal interactions that formerly contributed to their internal integrity, lowering their stability. We note that, although penicillinase activity has been reduced by 100-fold in many of the ESBLs, these enzymes remain quite active against penicillins. It may be that in a clinical environment, where penicillins are widespread and where these enzymes have evolved, only so much penicillinase activity can be sacrificed. The need to maintain some penicillinase activity as cephalosporinase activity is evolved may be a relatively stringent constraint on the allowed substitutions. Consistent with this view, several studies have shown that more mutant enzymes are found when selected against only a single antibiotic than are found in the clinic, presumably reflecting the fewer functional constraints in the *in vitro* experiments.[8,18,23–26] Similarly, the lower stability of the mutant ESBL enzymes is tolerated for activity gain,[24,27] but appears to be

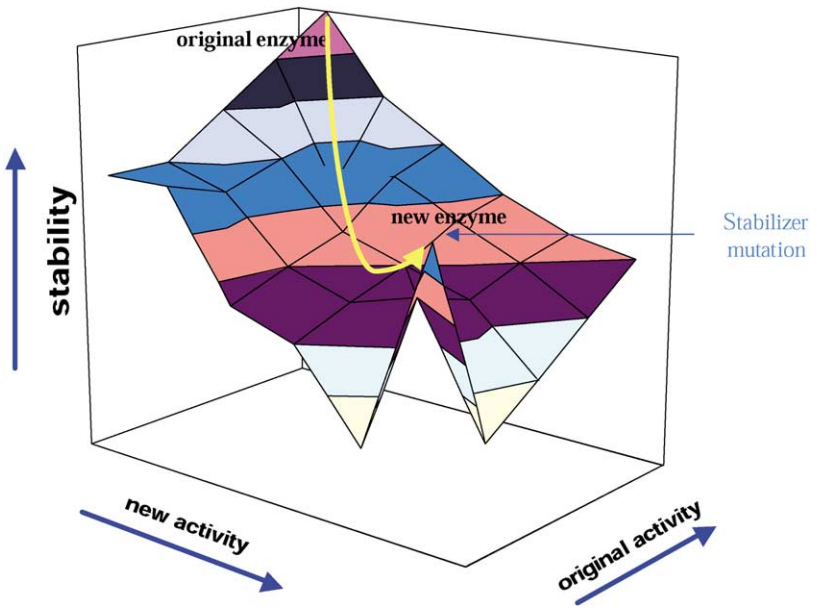

Figure 6. Proposed relationship between new activity, original activity, and protein stability.

disadvantageous.[25] The low-stability ESBLs confer less resistance at higher temperatures, and a secondary substitution (M182T) is often further selected, both naturally and by *in vitro* evolution, to restore stability.[14,17,26]

The model that emerges is summarized in Figure 6. As TEM mutant enzymes have gained cephalosporinase activity, they have sacrificed penicillinase activity and thermodynamic stability. We note that the evolutionary path may be oversimplified; what appear to be functionally neutral stabilizing substitutions, such as M182T, maybe present from the start as a polymorphism in bacterial populations. Still, on the basis of its later emergence (judged by higher TEM numbers and later round appearance in *in vitro* evolution studies[14,17,26,28]), we suspect that Met182 → Thr is indeed a late-appearing, secondary substitution. In either case, it seems clear that stability is selected evolutionarily. Although function is the most important thing selected[8,23] for even a relatively small loss of stability (2–3 kcal mol^{-1}) appears to confer a selective disadvantage compared to an iso-functional, stabilized enzyme. Other enzymes, such as HIV protease and DNA gyrase B, may undergo the same pattern of substitutions that gain function but lose stability, followed by a restoring substitution (Figure 6).[29,30] Such stabilizing substitutions may help to explain substitutions far from active sites that are often observed in evolving resistance enzymes.

Methods

Site-directed mutagenesis, protein purification, and crystallization

Mutagenesis was carried out using a modified two-step PCR protocol;[16,31] mutation was verified by sequencing of the entire coding region. The mutant genes were transformed into a protease-deficient *E. coli* SF120 strain. The enzymes were purified in a procedure modified from that described by Dubus *et al*.[16,32] The protein was produced at RT in 2 × YT medium. Cells were collected by centrifugation and resuspended in buffer A (5 mM Tris–HCl, pH 8.0), containing 1 mM EDTA and 20% (w/v) sucrose in RT for ten minutes. Cells were then collected and resuspended in ice-cold 5 mM $MgCl_2$ for ten minutes. The supernatant was saved as the periplasmic contents, concentrated to about 100 ml, and dialyzed against buffer A. The crude extract was applied to a Q-Sepharose Fast Flow column (Pharmacia, Uppsala, Sweden) equilibrated with buffer A. The column was then washed extensively with buffer A. The enzyme was eluted by buffer A containing 100 mM NaCl. M182T was crystallized in buffer B (1.5 M sodium phosphate buffer, pH 8.0).[33] G238A (the TEM analog of SHV-13), and TEM-64 crystals were grown in buffer B in the presence of 2.5 mM transition-state analogs, compound **2** for G238A and compound **1** for TEM-64 (Figure 4(c) and (d)).[20] These transition-state analogs were added to facilitate crystal growth of these ESBL mutant enzymes.

Enzyme kinetics

Enzyme assays were performed in 50 mM sodium phosphate buffer (pH 7.0), at RT. FAP was purchased from Calbiochem (La Jolla, CA), CAZ was a gift from D. J. Blazquez, and CTX was purchased from Sigma (St Louis, MO). The extinction coefficients used were: TEM-1, $\varepsilon_{281} = 29,400\ \mathrm{cm^{-1}\,M^{-1}}$; FAP, $\varepsilon_{308} = 22,800\ \mathrm{cm^{-1}\,M^{-1}}$, $\Delta\varepsilon_{340} = 1730\ \mathrm{cm^{-1}\,M^{-1}}$; CAZ, $\varepsilon_{257} = 19,021\ \mathrm{cm^{-1}\,M^{-1}}$, $\Delta\varepsilon_{260} = 1730\ \mathrm{cm^{-1}\,M^{-1}}$; and CTX, $\varepsilon_{264} = 16,893\ \mathrm{cm^{-1}\,M^{-1}}$, $\Delta\varepsilon_{260} = 6710\ \mathrm{cm^{-1}\,M^{-1}}$. The kinetics parameters k_{cat} and K_M were determined by initial velocity non-linear regression analysis ($v_0 = k_{cat}{\cdot}S/(K_M + S)$) using KaleidaGraph (Synergy Software, Reading, PA).

Thermal denaturation

The enzyme was denatured by raising the temperature in 0.1 deg. C increments at a ramp rate of

2 deg. C/min in 200 mM potassium phosphate (pH 7.0), using a Jasco 715 spectropolarimeter with a Peltier-effect temperature controller and an in-cell temperature monitor. Denaturation was marked by an obvious transition in both the far-UV CD (223 nm) and fluorescence signals (maximum at 340 nm measured using a 300 nm cut-on filter). The fluorescence and CD signals were monitored simultaneously. All melts were reversible and apparently two-state.[13,16] The temperature of melting (T_m) and van't Hoff enthalpy of unfolding (ΔH_{VH}) values were calculated with EXAM.[34] The free energy of unfolding relative to WT was calculated using the method proposed by Schellman: $\Delta\Delta G_u = \Delta T_m \cdot \Delta S_u{}^{WT}$.[35] A positive value of $\Delta\Delta G_u$ indicates a stability gain, and a negative value indicates stability loss. The $\Delta S_u{}^{WT}$ was 0.43(±0.02) kcal mol^{-1} K^{-1}. We note that this equation begins to break down for large ΔT_m or $\Delta\Delta H_{VH}$ values. For cases such as D179G, D179N, and M182T, we calculated $\Delta\Delta G_u$ using the Gibbs–Helmholtz equation, comparing mutant enzyme with the WT at the melting temperature of the WT enzyme (51.5 °C) and at 37 °C.[16] Using this method, which, admittedly, still retains some error owing to the uncertainties in ΔC_p, the $\Delta\Delta G_u$ value of D179G decreased from 4.0 kcal mol^{-1}, using the Schellman method, to 2.0 kcal mol^{-1} at 51.5 °C but actually increased to 4.3 kcal mol^{-1} at 37 °C. The $\Delta\Delta G_u$ value of D179N decreased from 2.1 kcal mol^{-1}, using the Schellman method, to 1.4 kcal mol^{-1} at 51.5 °C but at 37 °C increased to 3.0 kcal mol^{-1}. The $\Delta\Delta G_u$ of M182T was very similar by both calculations at both 51.5 °C and at 37 °C. What these differences reflect are different temperature dependences of the stability of a few of these mutant enzymes. Thus, the $\Delta\Delta G_u$ value will vary depending on the temperature at which it is evaluated. For these few enzymes, D179G and D179N most prominent among them, the quantitative values of $\Delta\Delta G_u$ are highly sensitive to temperature and, moreover, we suspect that their errors will be significant owing to changes in ΔC_p that we have not modeled. These considerations should not obscure the fact that mutants like D179G and D179N are quite destabilized relative to WT TEM-1 at all temperatures.

Disk diffusion assay

The procedure for the disk diffusion assay followed standards published by NCCLS, 1997 (vol. 17(1), M2–A6). Plasmids containing TEM-1 mutation were transformed into *E. coli* strain JM109. An overnight bacteria culture was diluted to A_{625} 0.1. Bacteria were striped on Mueller–Hinton agar plates (Becton Dickinson, Sparks, MD). Three antibiotic disks, CAZ30 (30 μg of ceftazidime) and CTX30 (30 μg of cefotaxime), and AM10 (10 μg of ampicillin, BBL™ Sensi-Disc™, Becton Dickinson), were placed at least 24 mm apart on plates. Five independent experiments were carried out for each mutant strain at each temperature. The diameter of inhibition zones (halo) was measured, including 6 mm of the drug disk itself. Smaller inhibition halos indicate more active enzymes. The standard error is less than 1 mm for all experiments.

X-ray data collection, structure determination and refinement

A crystal was mounted in a nylon loop and flash-frozen in a nitrogen stream (100 K). The X-ray diffraction data were collected on the 5-ID beamline (λ = 1.0000 Å) of the DND-CAT at the Advanced Photon Source (Argonne, IL) using a MARCCD detector. Data were processed in the DENZO/SCALEPACK suite[36] to 1.75, 1.85, and 1.80 Å resolution for M182T, G238A, and TEM-64, respectively (Table 6). Structures were solved by the program AMoRe[37] using TEM-1 (PDB code 1BTL[38]) as a search model. Crystallographic refinement was conducted with the program CNS[40] and followed by manual corrections in Turbo (Cambillau, C. & Roussel, A. (1997). *Turbo Frodo*, OpenGL edit., Universite Aix-Marseille II, Marseille, France) to final R_{cryst}/R_{free} values of 18.6/22.0% for M182T, 16.5/20.3% for G238A, and 16.8/18.9% for TEM-64 (Table 6).

Protein Data Bank accession codes

The coordinates for all structures have been deposited in the RCSB Protein Data Bank. The accession codes for TEM-1 M182T, G238A, and TEM-64 are 1JWP, 1JWV, 1JWZ, respectively.

Acknowledgments

This work was supported by NSF MCB-9734484 to B.K.S. We thank J. Blazquez for several ESBL constructs, W. Anderson and J. Brunzelle for technical advice, and E. Silinsky, A. Gross, B. Beadle, I. Trehan, R. Powers and J. Irwin for reading the manuscript. The DuPont-Northwestern-Dow CAT at APS is supported by DuPont Co., the Dow Chem. Co., the NSF and the State of Illinois.

References

1. Richards, F. M. (1977). Areas, volumes, packing, and protein structure. *Annu. Rev. Biophys. Bioeng.* **6**, 151–176.
2. Warshel, A., Aqvist, J. & Creighton, S. (1989). Enzymes work by solvation substitution rather than by desolvation. *Proc. Natl Acad. Sci. USA*, **86**, 5820–5824.
3. Warshel, A. (1978). Energetics of enzyme catalysis. *Proc. Natl Acad. Sci. USA*, **75**, 5250–5254.
4. Elcock, A. H. (2001). Prediction of functionally important residues based solely on the computed energetics of protein structure. *J. Mol. Biol.* **312**, 885–896.
5. Herzberg, O. & Moult, J. (1991). Analysis of the steric strain in the polypeptide backbone of protein molecules. *Proteins: Struct. Funct. Genet.* **11**, 223–229.
6. Meiering, E. M., Serrano, L. & Fersht, A. R. (1992). Effect of active site residues in barnase on activity and stability. *J. Mol. Biol.* **225**, 585–589.
7. Shoichet, B. K., Baase, W. A., Kuroki, R. & Matthews, B. W. (1995). A relationship between protein stability and protein function. *Proc. Natl Acad. Sci. USA*, **92**, 452–456.
8. Schreiber, G., Buckle, A. M. & Fersht, A. R. (1994). Stability and function: two constraints in the evolution of barstar and other proteins. *Structure*, **2**, 945–951.
9. Kidokoro, S., Miki, Y., Endo, K., Wada, A., Nagao, H., Miyake, T. *et al.* (1995). Remarkable activity enhancement of thermolysin mutants. *FEBS Letters*, **367**, 73–76.

10. Livermore, D. M. (1996). Are all beta-lactams created equal? *Scand. J. Infect. Dis. Suppl.* **101**, 33–43.
11. Knox, J. R. (1995). Extended-spectrum and inhibitor-resistant TEM-type beta-lactamases: mutations, specificity, and three-dimensional structure. *Antimicrob. Agents Chemother.* **39**, 2593–2601.
12. Massova, I. & Mobashery, S. (1998). Kinship and diversification of bacterial penicillin-binding proteins and beta-lactamases. *Antimicrob. Agents Chemother.* **42**, 1–17.
13. Raquet, X., Vanhove, M., Lamotte-Brasseur, J., Goussard, S., Courvalin, P. & Frere, J. M. (1995). Stability of TEM beta-lactamase mutants hydrolyzing third generation cephalosporins. *Proteins: Struct. Funct. Genet.* **23**, 63–72.
14. Huang, W. & Palzkill, T. (1997). A natural polymorphism in beta-lactamase is a global suppressor. *Proc. Natl Acad. Sci. USA*, **94**, 8801–8806.
15. Sideraki, V., Huang, W., Palzkill, T. & Gilbert, H. F. (2001). A secondary drug resistance mutation of TEM-1 beta-lactamase that suppresses misfolding and aggregation. *Proc. Natl Acad. Sci. USA*, **98**, 283–288.
16. Wang, X., Minosov, G. & Shoichet, B. K. (2002). Noncovalent interaction energies in covalent complexes: TEM-1 beta-lactamase and beta-lactams. *Proteins: Struct. Funct. Genet.* **46**, 86–96.
17. Orencia, M. C., Yoon, J. S., Ness, J. E., Stemmer, W. P. & Stevens, R. C. (2001). Predicting the emergence of antibiotic resistance by directed evolution and structural analysis. *Nature Struct. Biol.* **8**, 238–242.
18. Vakulenko, S. B., Taibi-Tronche, P., Toth, M., Massova, I., Lerner, S. A. & Mobashery, S. (1999). Effects on substrate profile by mutational substitutions at positions 164 and 179 of the class A TEM(pUC19) beta-lactamase from *Escherichia coli*. *J. Biol. Chem.* **274**, 23052–23060.
19. Taibi-Tronche, P., Massova, I., Vakulenko, S. B., Lerner, S. A. & Mobashery, S. (1996). Evidence for structural elasticity of class A β-lactamases in the course of catalytic turnover of the novel cephalosporin cefepime. *J. Am. Chem. Soc.* **118**, 7441–7448.
20. Caselli, E., Powers, R. A., Blasczcak, L. C., Wu, C. Y., Prati, F. & Shoichet, B. K. (2001). Energetic, structural, and antimicrobial analyses of beta-lactam side chain recognition by beta-lactamases. *Chem. Biol.* **8**, 17–31.
21. Herzberg, O., Kapadia, G., Blanco, B., Smith, T. S. & Coulson, A. (1991). Structural basis for the inactivation of the P54 mutant of beta-lactamase from *Staphylococcus aureus* PC1. *Biochemistry*, **30**, 9503–9509.
22. Chen, C. C., Rahil, J., Pratt, R. F. & Herzberg, O. (1993). Structure of a phosphonate-inhibited beta-lactamase. An analog of the tetrahedral transition state/intermediate of beta-lactam hydrolysis. *J. Mol. Biol.* **234**, 165–178.
23. Giver, L., Gershenson, A., Freskgard, P. O. & Arnold, F. H. (1998). Directed evolution of a thermostable esterase. *Proc. Natl Acad. Sci. USA*, **95**, 12809–12813.
24. Blazquez, J., Morosini, M. I., Negri, M. C. & Baquero, F. (2000). Selection of naturally occurring extended-spectrum TEM beta-lactamase variants by fluctuating beta-lactam pressure. *Antimicrob. Agents Chemother.* **44**, 2182–2184.
25. Axe, D. D. (2000). Extreme functional sensitivity to conservative amino acid changes on enzyme exteriors. *J. Mol. Biol.* **301**, 585–595.
26. Zaccolo, M. & Gherardi, E. (1999). The effect of high-frequency random mutagenesis on *in vitro* protein evolution: a study on TEM-1 beta-lactamase. *J. Mol. Biol.* **285**, 775–783.
27. Huang, W., Petrosino, J., Hirsch, M., Shenkin, P. S. & Palzkill, T. (1996). Amino acid sequence determinants of beta-lactamase structure and activity. *J. Mol. Biol.* **258**, 688–703.
28. Stemmer, W. P. (1994). Rapid evolution of a protein *in vitro* by DNA shuffling. *Nature*, **370**, 389–391.
29. Condra, J. H., Schleif, W. A., Blahy, O. M., Gabryelski, L. J., Graham, D. J., Quintero, J. C. *et al.* (1995). *In vivo* emergence of HIV-1 variants resistant to multiple protease inhibitors. *Nature*, **374**, 569–571.
30. Blance, S. J., Williams, N. L., Preston, Z. A., Bishara, J., Smyth, M. S. & Maxwell, A. (2000). Temperature-sensitive suppressor mutations of the *Escherichia coli* DNA gyrase B protein. *Protein Sci.* **9**, 1035–1037.
31. Ho, S. N., Hunt, H. D., Horton, R. M., Pullen, J. K. & Pease, L. R. (1989). Site-directed mutagenesis by overlap extension using the polymerase chain reaction. *Gene*, **77**, 51–59.
32. Dubus, A., Wilkin, J. M., Raquet, X., Normark, S. & Frere, J. M. (1994). Catalytic mechanism of active-site serine beta-lactamases: role of the conserved hydroxy group of the Lys-Thr(Ser)-Gly triad. *Biochem. J.* **301**, 485–494.
33. Strynadka, N. C., Adachi, H., Jensen, S. E., Johns, K., Sielecki, A., Betzel, C. *et al.* (1992). Molecular structure of the acyl-enzyme intermediate in beta-lactam hydrolysis at 1.7 Å resolution. *Nature*, **359**, 700–705.
34. Kirchoff, W. (1993). EXAM: A two-state thermodynamic analysis program, Gaithersburg, Maryland
35. Becktel, W. J. & Schellman, J. A. (1987). Protein stability curves. *Biopolymers*, **26**, 1859–1877.
36. Otwinowski, Z. & Minor, W. (1997). Processing of X-ray diffraction data collected in oscillation mode. *Methods Enzymol.* **276**, 307–326.
37. Navaza, J. (1994). AMoRe – an automated package for molecular replacement. *Acta Crystallog. sect. A*, **50**, 157–163.
38. Jelsch, C., Mourey, L., Masson, J. M. & Samama, J. P. (1993). Crystal structure of *Escherichia coli* TEM1 beta-lactamase at 1.8 Å resolution. *Proteins: Struct. Funct. Genet.* **16**, 364–383.
39. Fonze, E., Charlier, P., Toth, Y., Vermeire, M., Raquet, X., Dubus, A. & Frere, J. M. (1995). TEM-1 β-lactamase structure solved by molecular replacement and refined structure of the S235A mutant. *Acta Crystallog. sect. D*, **51**, 682–694.
40. Brünger, A. T., Adams, P. D., Clore, G. M., DeLano, W. L., Gros, P., Grosse-Kunstleve, R. W. *et al.* (1998). Crystallography and NMR system: a new software suite for macromolecular structure determination. *Acta Crystallog. sect. D*, **54**, 905–921.

Edited by R. Huber

(Received 19 December 2001; received in revised form 18 March 2002; accepted 15 April 2002)